Proceedings of the 21th Symposium of the International Committee on Aeronautical Fatigue, June 27-29, 2001, Toulouse, France.

CRACK BULGING EFFECTS IN LONGITUDINAL CRACKS IN PRESSURIZED NARROW BODY AIRCRAFT

∗ Catherine A. Bigelow
∗John G. Bakuckas, Jr.
∗ Paul W. Tan
∗Xiaogong Lee,
and
**Anisur Rahman

Abstract: Longitudinal cracks in pressurized aircraft fuselages are subjected to hoop load and bending. The interaction of these two loadings results in the so-called "bulging effect," which can significantly elevate the stress-intensity factor at the crack tip and reduce the residual strength. The damage tolerance design philosophy requires realistic stress state determination in the vicinity of cracks in airframe fuselages. However, few studies have been done to study the significance of bulging effects for cracks in a narrow-body fuselage representative of commuter aircraft and the consequence of not including these effects in the stress predictions and subsequent damage tolerance analysis. Of particular concern is the effect of bulging in a fuselage that has been repaired. Repair adds new flaw initiation sites to the structure and can also alter the bulging response of the fuselage. To examine the effects of bulging on stress-intensity factor and residual strength calculations in a repaired structure, the Federal Aviation Administration is studying the bulging effects in narrow-body aircraft fuselages. Bulging factors were calculated using a nonlinear finite element analysis. The stress-intensity factors at the crack tip were calculated using the Modified Crack Closure Integral method. In this study, a cutout was placed in a narrow-body aircraft fuselage and was repaired by an internal doubler attached with rivets. A crack was positioned in the critical rivet row. Typical results from the study are presented and the effects on the bulging factor of varying different parameters, such as loading, crack length, and the presence of stiffeners, are discussed.

INTRODUCTION

In December 1978, the Federal Aviation Administration (FAA) amended their requirements to include a damage tolerance philosophy. The damage tolerance approach relies on accurate crack growth predictions, which require accurate stress-intensity factor

∗ FAA William J. Hughes Technical Center, AAR-430, Atlantic City International Airport, NJ, USA.

** Drexel University, Department of Materials Engineering, Philadelphia, PA, USA.

(SIF) calculations. Longitudinal cracks in cylindrical pressure vessels, such as an aircraft fuselage, can exhibit out-of-plane deformation or bulging. Bulging is caused by local bending of the crack faces as a result of loss of hoop stress in the vicinity of the crack tip [1]. The bulging deformation leads to an increase in the crack tip energy release rate, and hence an increase in the SIF. The SIF is commonly used as the basis of quantifying the bulging phenomenon. In this work, the bulging effect is quantified by the bulging factor, which is defined by (1):

$$\beta = \frac{K_{I\,curved}}{K_{I\,flat}} \tag{1}$$

Here, $K_{I\,curved}$ is the Mode I SIF for a crack in the curved panel, and $K_{I\,flat}$ is the Mode I SIF for the same crack in an infinite flat panel under a remote tension equal in value to the hoop stress in the curved panel. Thus the bulging factor, β, is a geometry factor, which can be applied to the SIF of a flat plate to obtain the SIF for a curved shell with the same crack. To accurately determine the effect of crack bulging on crack growth in curved structures, calculations of the bulging factors for the fuselage configurations used in industry are needed.

Most work done to date has been for unstiffened shells. In an unstiffened cylindrical shell, it has been shown that the bulging factor will increase monotonically with an increase in crack length, decrease with an increasing radius of curvature and shell thickness, and decrease with increasing internal pressure. Comparisons with experimental results indicate that bulging is a nonlinear phenomenon and is over-predicted by a linear analysis [1, 2]. In a built-up structure like a fuselage, however, the crack interacts with the stiffening elements and the position of the crack relative to the stiffening elements becomes an important parameter in determining the influence of bulging. A few studies have been done for stiffened shells [1, 3, 4]. In general the stiffening elements carry a portion of the load, thus reducing the stresses in the skin. The reduction of the stress is less in areas of skin away from the stiffeners, such as in mid-bay, and greater closer to the stiffening elements. The bulging factor has been calculated to be between 0.4 and 1.8 for built-up stiffened fuselage structures typical of large transport aircraft [1, 4]. In stiffened structures the bulging factor accounts for the effect of curvature and the distribution of the load between the skin and stiffeners. The first results in an increase in the value of the SIF and the latter a decrease. Thus, a value less than unity indicates that the effect of stiffeners in reducing the SIF prevailed over the effect of curvature in increasing the SIF.

The published work on bulging effects in fuselages of commuter class aircraft is very limited. However, the problem is no less important for this category of aircrafts than in transport category aircraft. Commuter planes often have a smaller fuselage radius and operate at lower internal pressures than transport planes. Both these parameters tend to increase the bulging factor in unstiffened shells. The bulging effect is also important in analyzing a repaired fuselage. Having a hole or a cutout in the fuselage which requires a repair will tend to increase the bulging factor, whereas the repair patch itself will add to the stiffness of the fuselage and thus decrease the bulging factor. No solutions for bulging factors for a repaired fuselage configuration exist. In the current study, a typical fuselage and repair configuration were selected. A crack was placed in the critical rivet row and bulging factors were calculated for various crack lengths. The effects of the presence of the repair patch, the longerons, and the frames on the bulging factor were examined. The

current results will help in evaluating the need to incorporate bulging factors in the design of repairs of commuter category aircraft

COMPUTATIONAL METHODOLOGY

Modified Crack Closure Integral (MCCI) Method

In this study, the Modified Crack Closure Integral (MCCI) method was used to calculate the SIF. In the MCCI method, it is assumed that the energy released during crack extension is the same as the work that would be needed to close the crack and that the energy released can be partitioned into four components of SIF [5-7]. The four SIF components consists of two in-plane stress-intensity factors, K_1, and K_2, due to the opening or tension mode and the shearing mode, respectively. The other two stress-intensity factors, k_1, and k_2, called the Kirchoff stress-intensity factors are due to the symmetric bending and unsymmetric bending loads, respectively. The loading modes are shown in Figure 1. The MCCI method approximates the work needed to close the crack using the local crack-tip displacements and forces. The displacements and forces at the nodes of the four elements surrounding the crack tip were obtained from the finite element results for each crack length, as shown in Figure 2. The work, W_i, done to close a crack of length, Δa, for the ith degree of freedom is given by [6]:

$$W_i = \frac{1}{2t\Delta a}\left[F_i^{close}\left(u_i^{top} - u_i^{bot}\right)\right], i = 1,\ldots,6 \tag{2}$$

where, t is the thickness of the panel, F is the force needed to close the crack surfaces, u is the displacement component on each node on the surface of the crack, and i denotes the degree of freedom. The total amount of work necessary to close a crack by Δa is numerically equal to the total amount of strain energy released when the crack grows by Δa. The strain energy release rate is related to the SIF using the following mapping:

$$W_2 + W_6 = \frac{K_1^2}{E} \tag{3}$$

$$W_1 = \frac{K_2^2}{E} \tag{4}$$

$$W_4 = \frac{k_i^2 \pi}{3E}\left(\frac{1+\nu}{3+\nu}\right) \tag{5}$$

and,

$$W_3 + W_5 = \frac{k_2^2 \pi}{3E}\left(\frac{1+\nu}{3+\nu}\right) \tag{6}$$

Only the mode I SIF, K_1, was used to calculate the bulging factor, using equation (1).

Verification and Convergence Studies

To verify the computational approach and to insure sufficient fidelity in the finite element mesh, a problem with known solution was modeled first: a pressurized unstiffened cylinder with a radius R of 64.96 in (1650 mm). The cylinder was made of 2024 aluminum alloy with a thickness t of 0.0394 in (1 mm). A longitudinal crack $2a$ = 7.874 in (200 mm) was modeled as shown schematically in Figure 3. The solution of this problem can be obtained from the work of Bakuckas [3] and Chen [2, 8]. Bakuckas solved the problem using nonlinear finite element method with global local hierarchical finite element approach and used the J-integral to calculate the SIF. Chen combined analytical results of Ansell [1] and Riks [4] with test results and presented the bulging factors in the form of a semi-empirical equation given by (7):

$$\beta = \sqrt{1 + \frac{5}{3\pi} \cdot \frac{Eta}{R^2 p} \cdot 0.316 \cdot \tanh\left(0.06 \cdot \frac{R}{t} \cdot \sqrt{\frac{pa}{Et}}\right)} \tag{7}$$

Here, E is the tensile modulus of the cylindrical shell, t is the thickness, R is the radius of curvature, p is the internal pressure, and a is the half crack length.

The model for the configuration shown in Figure 3 consisted of 17046, 4-noded, reduced integration shell elements and a total of 104010 degrees of freedom (dof). A geometrically nonlinear finite element analysis was conducted using the commercial finite element package ABAQUS [9]. Load was applied incrementally loading the model from 0 to 10 psi and the bulging factor was calculated at each increment. The mode I SIF obtained from the finite element analysis was used as $K_{I\ curved}$ in equation (1) to calculate the bulging factor. The SIF for a flat plate, $K_{I\ flat}$, was obtained from [10], and is given by:

$$K_{I\ flat} = \frac{pR}{t}\sqrt{\pi a} \tag{8}$$

Here, p is the internal pressure, R is the fuselage radius, and t is the skin thickness. Figure 4 shows the plot of the bulging factor as a function of pressure. The results show that the bulging factor decreases with increasing pressure. Thus, the bulging phenomenon is nonlinear, since linear theory would predict that the bulging factor is independent of internal pressure [11]. More importantly, the solutions are within 1% of the values reported by Bakuckas and that obtained from Chen's semi-empirical equation given by (7), thus verifying the approach used.

A convergence study was also done to insure that the finite element mesh used had sufficient fidelity. The study was conducted by developing two additional finite element meshes of the verification problem, one with a coarser mesh than that used in the verification analysis, and the other with a finer mesh. The bulging factor obtained by each of the three meshes as a function of pressure is depicted in Figure 5. These results show that the finite element model with coarser mesh has sufficient fidelity for the given problem.

Geometry and Configuration

Once the procedure was verified, the methodology was used to analyze bulging effects in a fuselage structure typical of a narrow body commuter category aircraft. In this study, for all analyses, a representative fuselage radius of 40 in. was used. Four fuselage configurations were considered. The first was an unstiffened fuselage with a longitudinal crack but with no repair. The second configuration was an unstiffened fuselage with a 6 in. × 8 in. cutout with 12 in. × 14 in. internal doubler repair. For the third and fourth configurations, a fuselage with a 6 in. × 8 in. cutout with 12 in. × 14 in. internal doubler repair was stiffened first longerons only and then with both longerons and frames, respectively. The four fuselage configurations are shown in Figure 6. The repair patch was attached to the fuselage with three rows of rivets with a 1 in. pitch. The repair is shown schematically in Figure 7. The stiffeners were also attached with rivets with a 1 in. pitch. The skin and the repair were made of 2024 aluminum alloy with a thickness of 0.04 in. The longeron (longitudinal stiffeners) had a hat cross-section; the stringers (hoop stiffeners) had a Z cross-section. The cross-sectional area of the longerons and the stringers were 0.1336 in.^{2} and 0.20 in.^{2}, respectively. The longerons were spaced at 9 in. intervals, and the stringers were spaced 18 in. apart.

Four different crack lengths were modeled in fuselage configuration. The half crack lengths were 2.1 in., 4.2 in., 7 in. and 8.2 in. These lengths correspond to a/L ratios of 0.3, 0.6, 1.0, and 1.2, where a is the half-crack length, and L is half length of the repair in the longitudinal direction. A total of 16 different cases were analyzed. In the first, or baseline, configuration the longitudinal crack was placed in the center of the panel. In the other fuselage configurations with repairs, the longitudinal crack was placed centrally along the critical rivet row, i.e., the outermost rivet row. The crack is shown schematically in Figure 7. The rivets at locations on the crack were assumed to be completely broken.

RESULTS AND DISCUSSION

All results in this work are presented in terms of bulging factor plots. In these plots the bulging factor, β, is plotted as a function of applied internal pressure. The bulging factor β is calculated for a given fuselage configuration and crack length using only the mode I component SIF normalized by the SIF of an identical crack in an infinite flat plate under remote tension equal to the hoop stress in the given configuration.

The first set of analyses is for the baseline configuration, an unstiffened fuselage with a central crack. The bulging factor for this configuration is plotted as a function of internal pressure in Figure 8. Results show that for all crack lengths, the bulging factor decreases as pressure increases. This has been attributed to the straightening or tightening of the crack in the hoop direction as the pressure increases and the same effect has been reported for large transport category aircraft by other authors [1, 3, 4, 8]. The variation in bulging factor increases as the crack length increases. For the smallest crack length analyzed (a=2.1 in., where a is the half crack length), the bulging factor varies between 2.2 and 2.0, whereas for the longest crack length analyzed (a= 8.4 in.), the bulging factor varies

between 6.2 and 4.2. Thus, the bulging phenomenon in unstiffened cylindrical shells becomes more nonlinear as the crack grows.

Figure 9 depicts the results for the analyses of the unstiffened fuselage configuration with a cutout repaired by internal doubler. In the longitudinal direction, the half length of the cutout is 4 in., and the half length of the repair patch is 7 in. Thus, for the shortest crack length (a=2.1 in., a/L=0.3), the crack is completely under the repair patch and is shorter than the longitudinal dimension of the cutout. For the next crack length (a=4.2 in., a/L=0.6), the crack is under the repair patch but is longer than the longitudinal dimension of the cutout, i.e., the crack tips extend past the ends of the cutout. The two larger cracks (a=7.0 in. and 8.4 in., a/L=1.0 and 1.2.) are equal to and longer than the repair patch, respectively. There are two competing mechanisms influencing the bulging factors in this case. The cutout decreases the stiffness of the fuselage, which increases the bulging factor. In opposition, the repair patch increases the rigidity of the fuselage and, hence, decreases the bulging factor. For the smallest crack length (a/L=0.3), the presence of the repair patch and the rivets results in about 30% reduction in bulging factor compared to the crack of same length in the unstiffened shell without the repair patch. This substantial decrease can be attributed to load redistribution around the cutout. The crack is in effect shielded from the load by the cutout and the presence of the two rows of rivets is not sufficient to redistribute any load into the crack region. At the longer crack length of $2a$=8.4 in., where additional rivets are broken, the upper crack face deforms or bulges out substantially more than the lower crack face, which is stiffened by the patch. Additionally, since the crack is just longer than the longitudinal dimension of the cutout, the crack tip is in a higher load zone. Thus bulging factor actually increases over that of the unstiffened shell by about 10 % at 1 psi and 27% at 10 psi for a/L=0.6. However, for the longer crack lengths, where the crack tip extends past the repair patch (a/L = 1.0, and a/L = 1.2), the internal pressure also has an effect on the behavior of the bulging factor. At lower pressures the bulging factor of the unstiffened shell without the repair is higher than the present case, but, at higher pressures, the values for the configuration with the patch are larger. Thus considering all crack lengths together we see that for the shortest crack, the bulging factor is smaller for the case of an unstiffened shell with a repair than for a similar crack in an unstiffened shell. For the other three crack lengths, the bulging factor is either larger or becomes larger at higher pressures for the case of an unstiffened shell with a repair. Thus a wide gap can be observed in Figure 9 between the curve for the shortest crack and the other three. Another observation one can make is that the dependence of bulging factor upon pressure is much weaker for the present case compared to the bulging factors for cracks in a unstiffened shell without a repair. This indicates that repair patch increases the stiffness to the point that the deformations are smaller and geometric nonlinearity is reduced.

Next set of analyses was for a fuselage with the same dimension as the previous configuration stiffened longitudinally by longerons. The results are shown in Figure 10. The presence of longerons provides additional stiffness to the configuration. Qualitatively the bulging factor values show similar trends as that of unstiffened shell without a repair (baseline configuration). However, the bulging factor values are lower and, also for the each crack length, the decrease in bulging factor as the load increases is much less. Here also the two smaller crack length (a/L=0.3 and 0.6) are fully underneath the repair patch, and the other two crack lengths (a/L=1.0 and 1.2) are equal to or extend beyond the repair patch. Thus, again the crack tips for the first two cracks are shielded from the load by the

cutout. We see that in Figure 10, the plots are not distributed evenly. The bulging factor plot for the first two crack lengths are grouped closer together, as are the other two curves. The presence of the longerons adds some stiffness to the configuration (overall lower bugling factors compared to the previous case), but doesn't affect the load redistribution around the cutout.

In the final set of analyses, the fuselage was stiffened in both the longitudinal and hoop directions. The bulging factors for this configuration are presented as a function of pressure in Figure 11. Frames added additional stiffening of the fuselage and reduced bulging factor compared to the results obtained in the previous case with longerons only. The effect of the frames increased for longer crack lengths. For the smallest crack analyzed, $a/L = 0.3$ ($a/L_{frame} = 0.2333$), β was reduced by less than 1% at $p = 1$ psi and by 2% at 10 psi compared to the case with a repair and longerons only. Here, L_{frame} is the half distance between two frames and $L/L_{frame} = 0.778$. For $a/L = 0.6$ ($a/L_{frame} = 0.4667$), the reduction in β ranged between 2% and 3% in the same pressure range. For larger cracks, when the crack tip is closer to the frame, we see a greater reduction of the bulging factor. For, $a/L = 1$ ($a/L_{frame} = 0.7778$), we see a drop of 37% and for $a/L = 1.2$ ($a/L_{frame} = 0.9333$), the reduction is almost 45%. In comparing this case (the repaired fuselage stiffened with both longerons and frames) with the previous case of the repaired fuselage stiffened with longerons only, we can see that the addition of the frames make this configuration stiffer and also increases the load transfer into the crack region. The absolute value of the bulging factor ranges from 1.1 to 1.6. Thus, bulging effect is still significant and should not be overlooked. There are two competing mechanisms in the determination of the bulging factor, as the crack length, a, increases, the bulging factor increases. However, as the crack approaches the frame, the bulging factor decreases. Thus we see, the bulging factor first increase and then decreases as a/L increases. As the crack length is increased the problem becomes more nonlinear, especially at lower pressures, so some exceptions to this rule is observed. At higher pressure when the structure "stretches" these exceptions resolves itself.

Figures 12 and 13 summarize the effect of configuration on the bulging factor. Figure 12 compares the bulging factor results for $a = 4.2$ in. ($a/L = 0.6$), the smallest crack length analyzed. As explained previously, the highest values of bulging factor are obtained for the unstiffened shell with a repair. The bulging factor decreases substantially when the fuselage is stiffened with longerons. However, there is only an incremental reduction in bulging factor by adding frames with the longerons. In this case the crack is too small and too far from the frames to be affected by it. Figure 13 shows the effect of configuration for a crack with a=8.4 in. (a/L=1.2), the longest crack length analyzed. In this case the crack is long enough to be influenced by the frame and there is a significant reduction in the bulging factor for the case with both longerons and frames compared to the case with just longerons. Additionally, for this crack length, the unstiffened, unrepaired case has the high bulging factors at lower pressures. At higher load pressures, the two unstiffened configurations with and without a repair have similar values for the bulging factors. This effect is due to the increased load transfer introduced by the frames at the longer crack length.

CONCLUDING REMARKS

The objective of this study was to determine the effects of bulging in aircraft structures representative of commuter aircraft. Typical configurations were chosen and analyzed. The Modified Crack Closure integral (MCCI) method was used to calculate crack-tip stress-intensity factors. The MCCI method was easy to use and the results were shown to be identical to those obtained by other methods. Parametric studies were done to examine various parameters and their effect on the bulging factor. For an unstiffened shell with a crack and a repair patch, the bulging factors were larger than for the baseline configuration of a crack in an unstiffened shell without a cutout or repair. The presence of the stiffeners significantly reduced the bulging factor but not to the level that it can be neglected. Bulging factors were calculated by considering the mode I component of the stress-intensity factor only. However, bulging in a stiffened structure and repair involves mode III deformations. Also it does not separate the contribution to bulging factor of the curvature and stiffening elements. While bulging factors are useful and widely used, there could be other ways of quantifying bulging and that is the subject of continuing research.

ACKNOWLEDGEMENT

This work was partially supported by National Computational Science Alliance and used the Silicon Graphics Origin 2000 Distributed Shared Memory System at University of Illinois at Urbana-Champain.

REFERENCES

[1] H. Ansell, "Bulging of Cracked Pressurized Aircraft Structure, *Tehnical Licentiate Dissertation*," in *Department of Mechanical Engineering*. Linkoping, Sweden: Linkoping Institute of Technology, 1988.

[2] D. Chen and J. Schive, "Bulging of Fatigue Cracks in Pressurized Aircraft Fuselages," Delft Institute of Technology, Delft, The Netherlands LR-655, May 1991.

[3] J. G. Bakuckas, P. V. Nguyen, C. A. Bigelow, and D. Broek, "Bulging Factors for Predicting Residual Strength of Fuselage Panels," in *Proceedings of the Symposium - International Committee on Aeronautical Fatigue*, vol. 1. Edinburgh, UK: EMAS, 1997.

[4] E. Riks, "Bulging Cracks in Pressurized Fuselages: A Numerical Study," National Aerospace Laboratories, Amsterdam, The Netherlands NLR MP 87058 U, November 17 1987.

[5] M. J. Viz, A. T. Zehnder, and J. D. Bamford, "Fatigue Fracture of Thin Plates Under Tensile and Transverse Shear Stresses," in *Fracture Mechanics: 26th Volume, ASTM STP 1256*, W. G. Reuter, J. H. Underwood, and J. James C. Newman, Eds. Philadelphia, PA: American Society for Testing and Materials, 1995.

[6] M. J. Viz, D. O. Potyondi, and A. T. Zehnder, "Computation of Membrane and Bending Stress-Intensity Factors for Thin Cracked Plates," *International Journal of Fracture*, vol. 72, pp. 21-38, 1995.

[7] E. F. Rybicki and M. F. Kanninen, "A Finite Element Calculation of Stress-Intensity Factors by a Modified Crack Closure Integral," *Engineering Fracture Mechanics*, vol. 9, pp. 931-938, 1977.

[8] D. Chen, "Bulging of Fatigue Cracks in a Pressurized Aircraft Fuselage," in *Department of Aerospace Engineering*. Delft, The Netherlands: Delft University of Technology, 1991.

[9] "ABAQUS," 5.8 ed. Pawtucket, RI 02860: Hibbitt, Karlsson, and Sorenson (HKS), 1998.

[10] Y. Murakami, *Stress intensity factors handbook*, 1st ed. Oxford [Oxfordshire]; New York: Pergamon, 1987.

[11] E. S. Folias, "The Stresses in a Cylindrical Shell Containing an Axial Crack," Office of Aerospace Research, Wright-Patterson Air Force Base, OH ARL 64-174, October 1964.

FIGURES

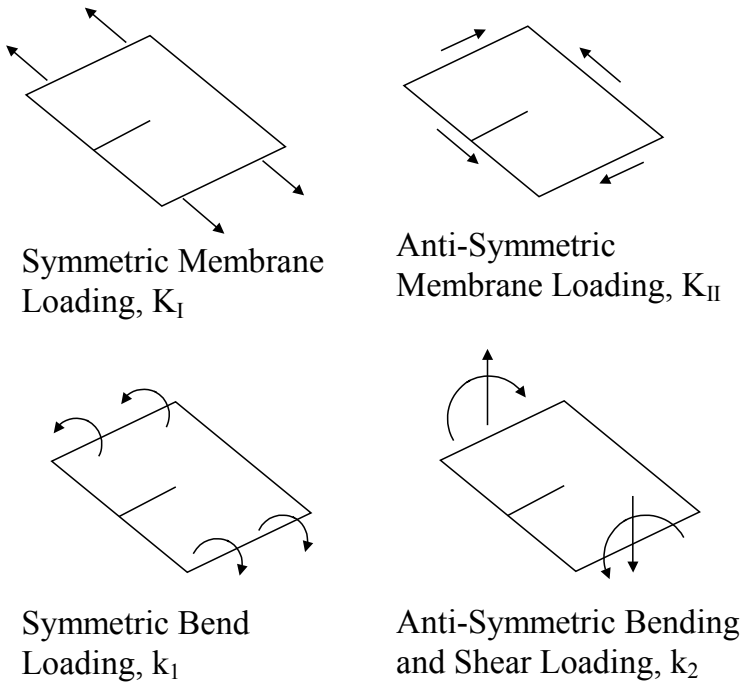

Figure 1 SIF modes for a plate

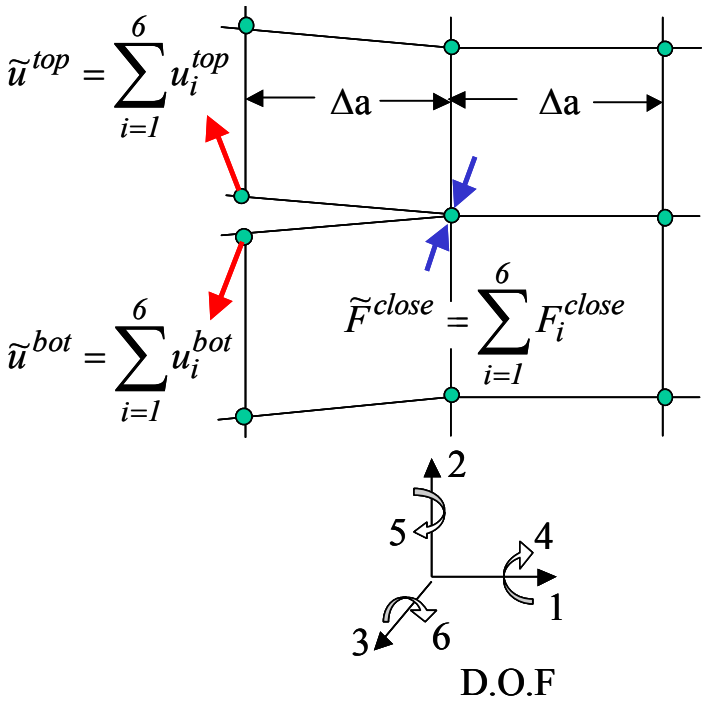

Figure 2 Crack tip forces and displacements needed for MCCI method

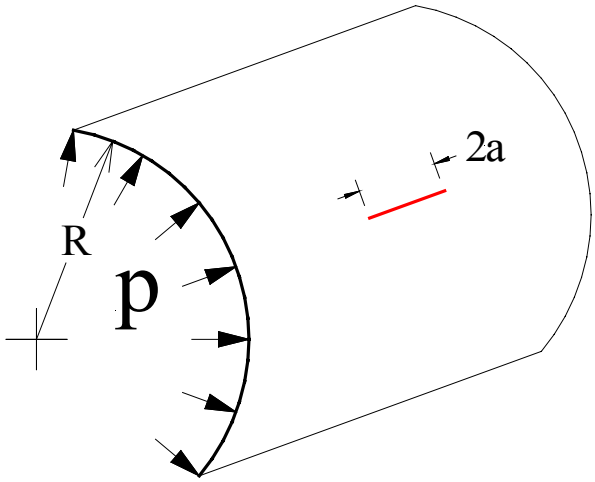

Figure 3 Configuration of the verification problem

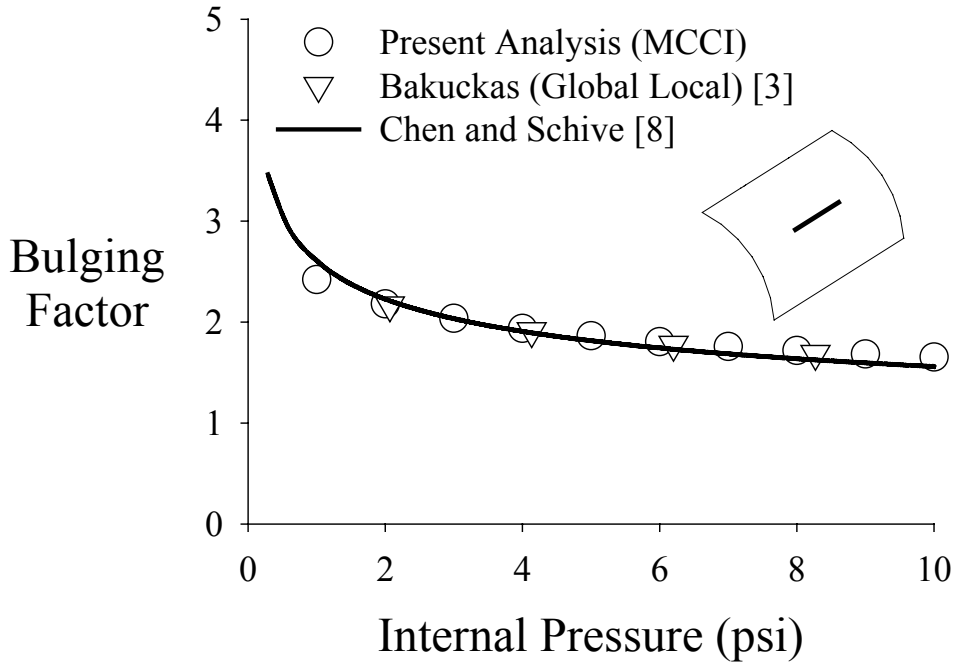

Figure 4 Comparison of bulging factor obtained by MCCI method with that obtained by other methods

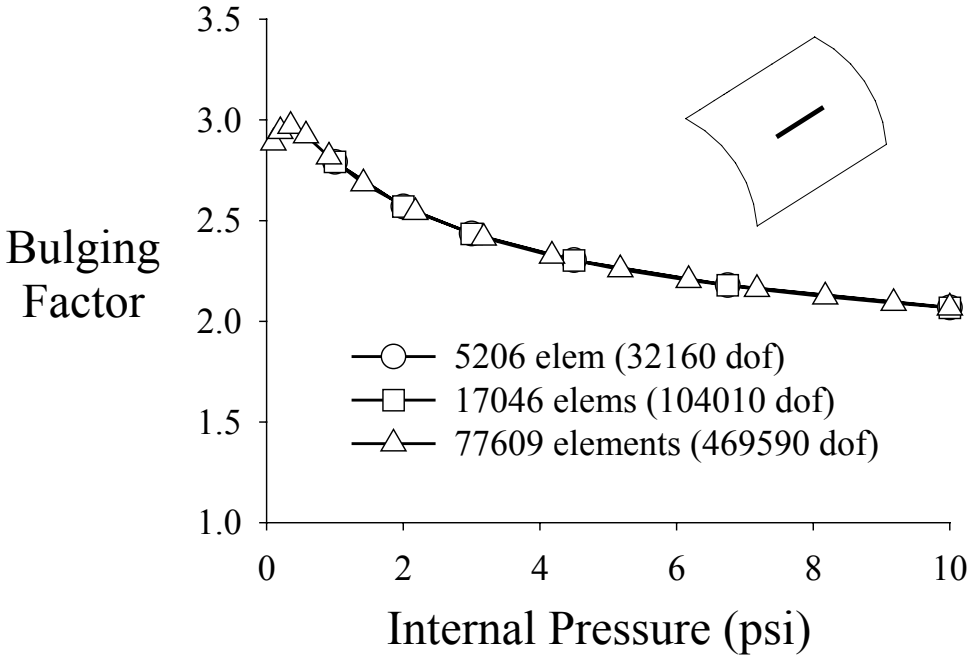

Figure 5 Mesh convergence test

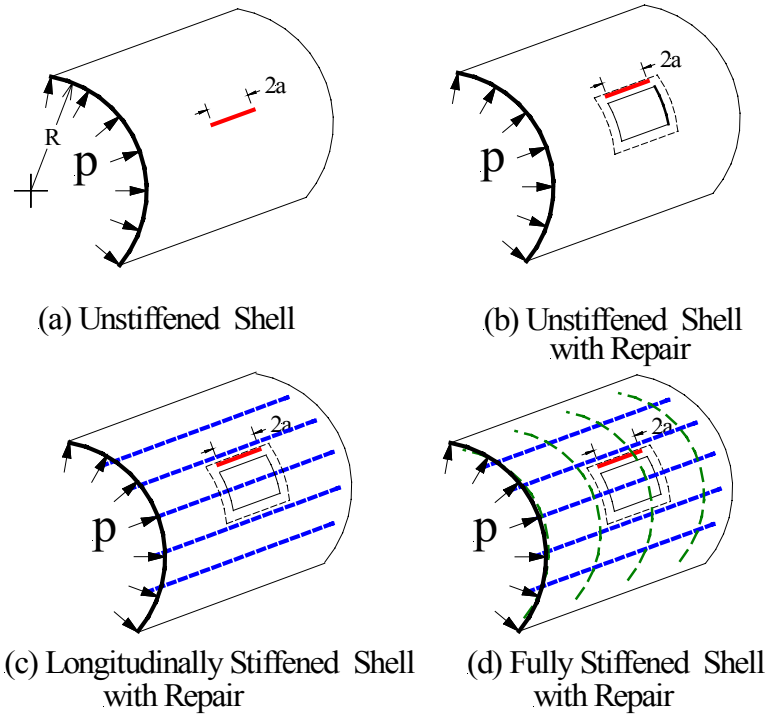

Figure 6 Fuselage configurations

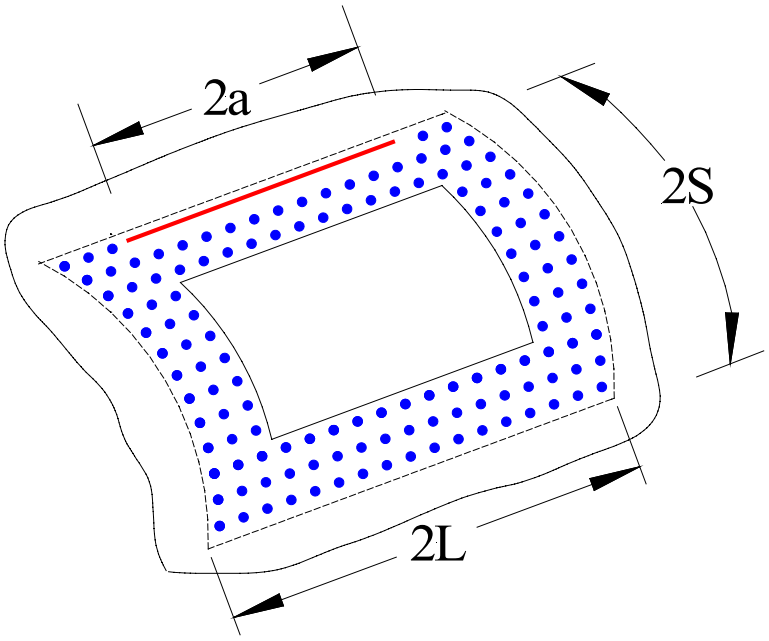

Figure 7 Details of the repair

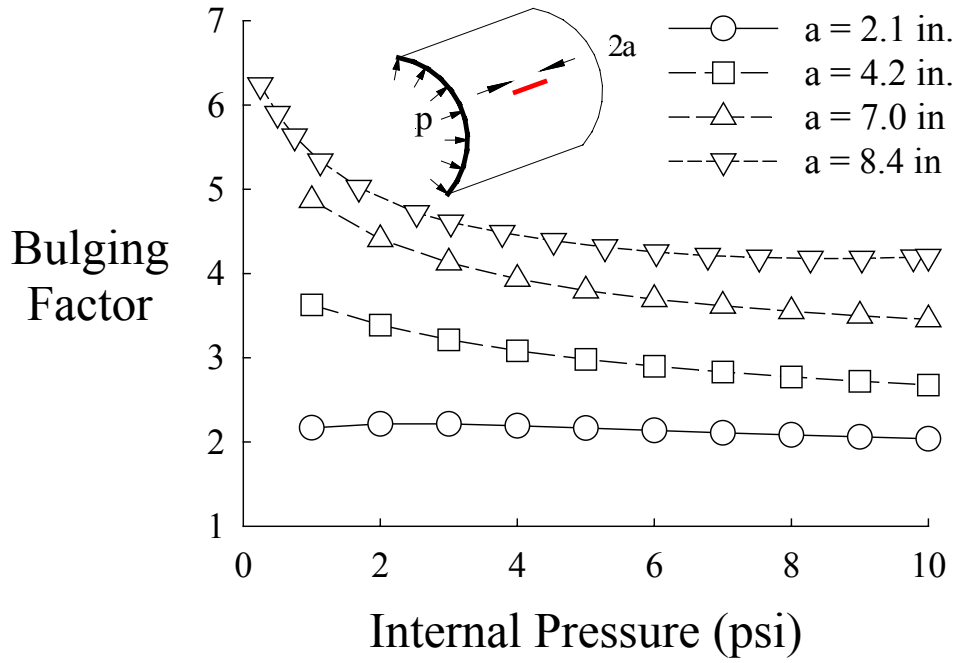

Figure 8 Bulging factors for longitudinal cracks in an unstiffened shell

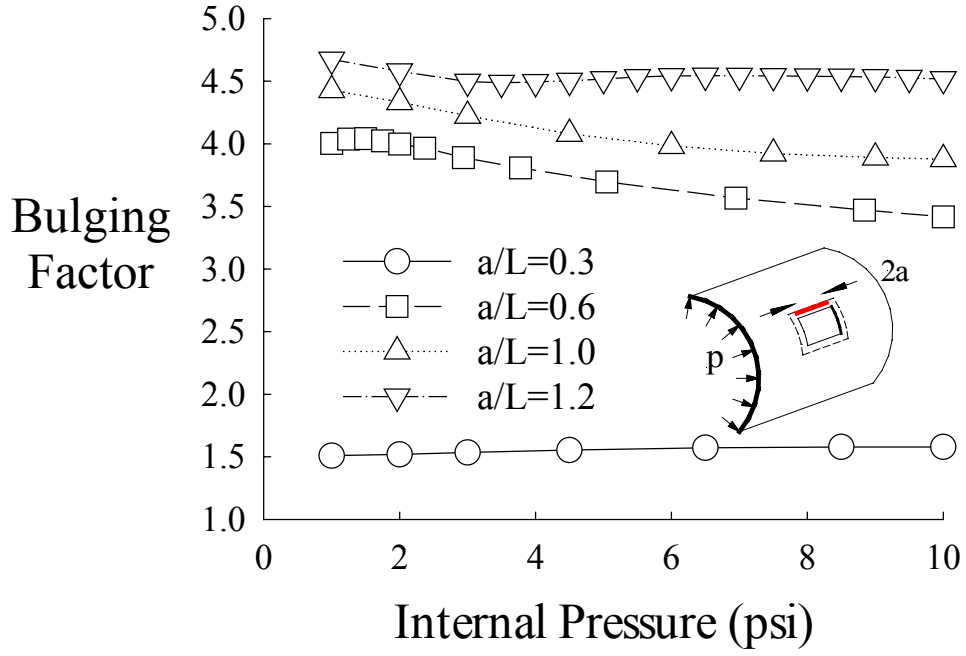

Figure 9 Bulging factor for a longitudinal crack in an unstiffened shell with repair

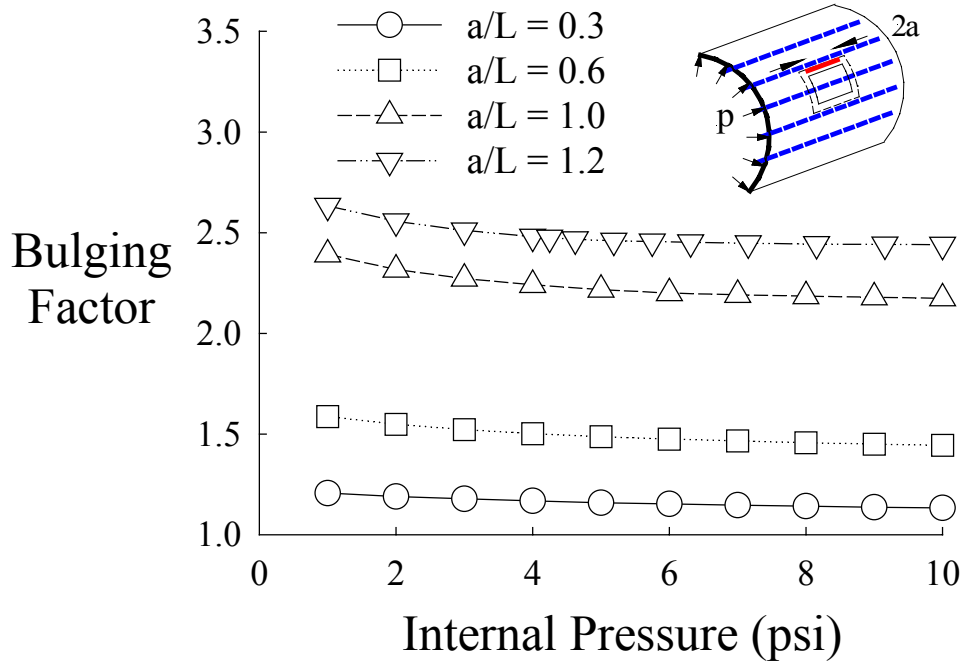

Figure 10 Bulging factor for a longitudinal cracks in a longitudinally stiffened shell with repair

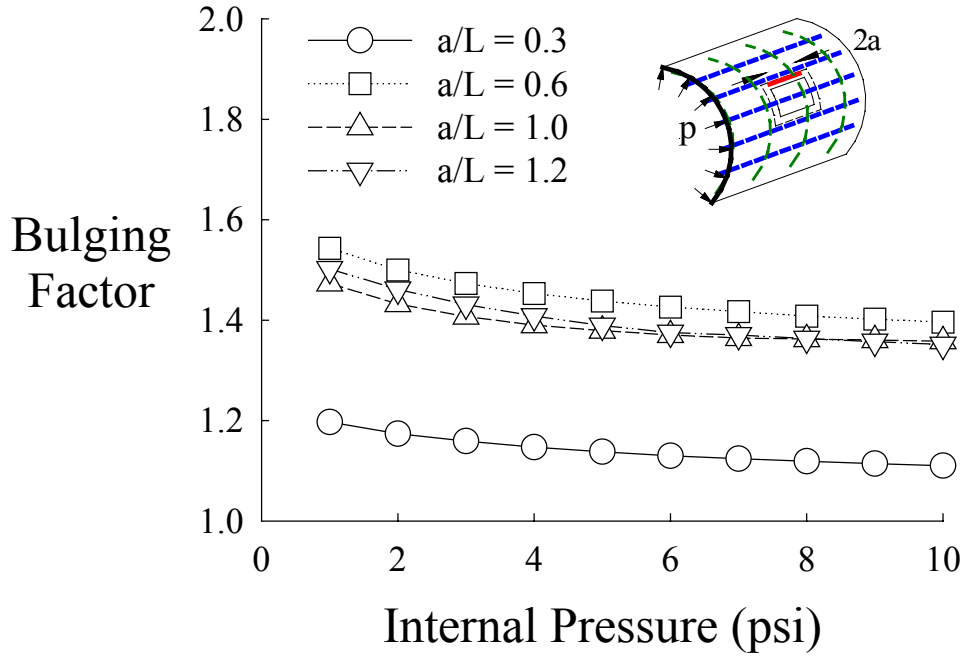

Figure 11 Bulging factors for longitudinal cracks in a shell stiffened with frames and longerons with a repair

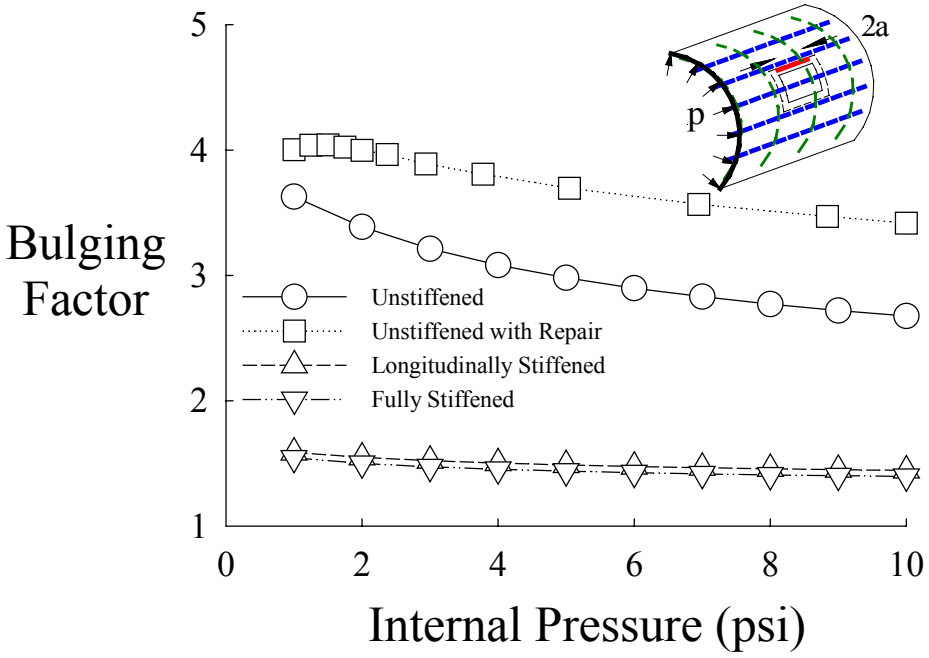

Figure 12 Effect of configuration on bulging factor, (a=4.2, a/L=0.6)

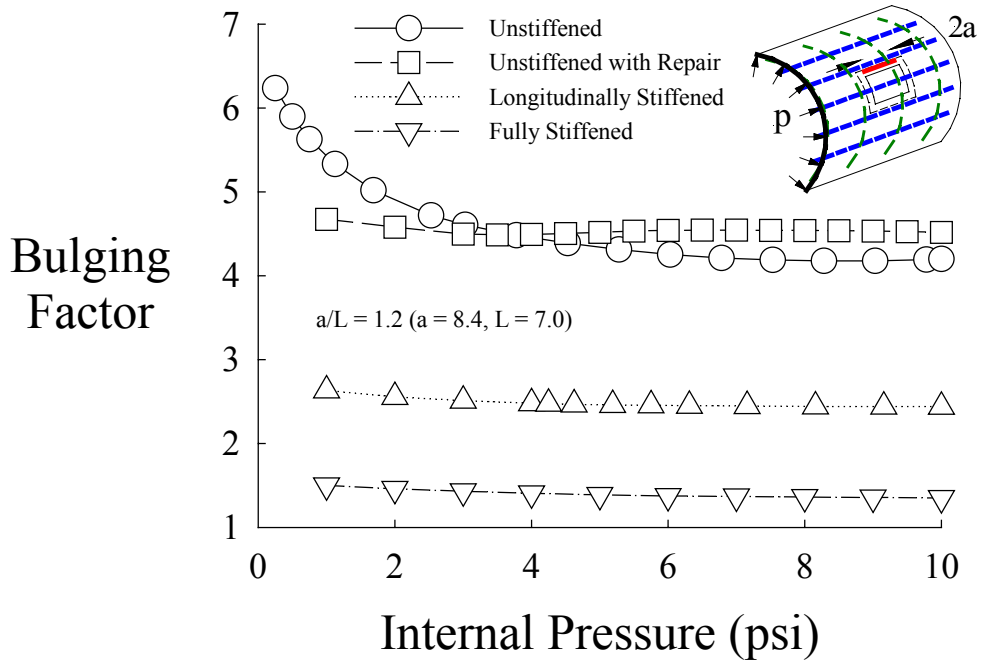

Figure 13 Effect of Configuration on bulging factor, (a=8.4, a/L=1.2)